

Article

Performance Comparison of Silicon- and Gallium-Nitride-Based MOSFETs for a Power-Efficient, DC-to-DC Flyback Converter

Osama Ahmed ^{1,2}, Yousuf Khan ^{1,*} , Muhammad A. Butt ^{3,4} , Nikolay L. Kazanskiy ^{4,5} 
and Svetlana N. Khonina ^{4,5} 

- ¹ Department of Electronic Engineering, Balochistan University of Information Technology, Engineering and Management Sciences, Airport Road, Quetta 87300, Pakistan; osama9240@gmail.com
² Design and Development, Elektro Control Industries, Sector I-11/4, Islamabad 44000, Pakistan
³ Institute of Microelectronics and Optoelectronics, Warsaw University of Technology, Koszykowa 75, 00-662 Warszawa, Poland; butt.m@ssau.ru
⁴ Image Processing Systems Institute, Samara National Research University, 443086 Samara, Russia; kazanskiy@ipsiras.ru (N.L.K.); khonina@ipsiras.ru (S.N.K.)
⁵ IPSI RAS-Branch of the FSRC “Crystallography and Photonics” RAS, 443001 Samara, Russia
* Correspondence: yousuf.naudhani@gmail.com

Abstract: Gallium Nitride (GaN)-based devices offer many advantages over conventional electronic devices, such as lower input/output capacitances, a higher switching speed, and a compact size, resulting in higher-density power outputs and reduced switching losses. This research investigates the power and switching efficiency of GaN-based FET in an active-clamp, DC-to-DC flyback converter for step-down application (24 V to 7 V) and compares it with silicon (Si)-based devices in the same circuit topology. The operation is analyzed under various input conditions and output loads such as R, RC, RL, and RLC. The proposed topology can achieve a maximum power-conversion efficiency of 99.6% and can operate at higher frequency values above 1 MHz. The presented GaN-based flyback model can replace conventional Si-based switches in power applications which require high power-efficiency and switching speed in a compact device.

Keywords: converter topology; flyback converter; GaN devices; high-frequency devices; power density; power efficiency



Citation: Ahmed, O.; Khan, Y.; Butt, M.A.; Kazanskiy, N.L.; Khonina, S.N. Performance Comparison of Silicon- and Gallium-Nitride-Based MOSFETs for a Power-Efficient, DC-to-DC Flyback Converter. *Electronics* **2022**, *11*, 1222. <https://doi.org/10.3390/electronics11081222>

Academic Editor: Kai Fu

Received: 23 February 2022

Accepted: 9 April 2022

Published: 12 April 2022

Publisher’s Note: MDPI stays neutral with regard to jurisdictional claims in published maps and institutional affiliations.



Copyright: © 2022 by the authors. Licensee MDPI, Basel, Switzerland. This article is an open access article distributed under the terms and conditions of the Creative Commons Attribution (CC BY) license (<https://creativecommons.org/licenses/by/4.0/>).

1. Introduction

Despite the advancements made in power electronic devices over the last two decades, conventional Si-based devices have reached their limits in terms of power efficiency, switching speed, and size. Insulated gate-based transistors (IGBTs) offered larger breakdown voltages and specific on-resistance [1], but they could not fulfill the requirement of modern, high-voltage applications. Recently, the focus of the research has been the discovery of new materials to improve the performance of power devices and make them more cost-effective, as compared to the existing, high-voltage, Si-based devices [2]. High performance and up-to-the-figure-of-merit-based gallium-arsenide (GaAs) power devices were developed in the 1980s to cope with the requirement of modern electronics, but they could not sustain the changing industry for long [3,4]. As technology moves towards miniaturization and the demand for power efficiency is on the rise, the effectiveness of any device will be judged on several merits, including threshold voltage, bandgap, stability of operation in harsh environments, immunity to high-voltage pulses and transient currents, low on-state resistance, and limited leakage currents [5]. Recently, nitride-based devices have drawn more attention for high power applications since the conventional Si-based devices cannot fulfill the requirement of modern power devices. The main nitride materials in group III include gallium nitride (GaN), aluminum nitride (AlN), and indium nitride (InN). These nitride materials can be used in high-temperature applications due to their improved material

properties, such as high electron mobility, sheet concentration, and larger breakdown area. Among nitrides, GaN has emerged as a promising candidate for semiconductor power devices with its material properties of a wide bandgap [6] and a larger breakdown voltage capacity. The interest in GaN grew in the late 1990s due to the introduction of a vast variety of applications in power-switching [7]. The GaN crystal is organized in a Wurtzite structure [8], having a hexagonal unit cell lacking inversion symmetry and enabling the material to acquire a very strong polarization effect. Additionally, GaN also offers material properties such as low on-resistance, lower switching losses, no body diode effect, low capacitance, low power consumption, and the ultimately small size of the device, resulting in lower fabrication costs. Table 1 lists the material properties of crucial semiconductor materials being used in power electronics. It can be seen that the bandgap energy for GaN (3.45 eV) is three times greater than that of Si (1.1 eV), making it a promising candidate for high-temperature operations. Moreover, the performance of the materials mentioned in Table 1 is compared in terms of Baliga's Figure of Merit (BFOM), which predicts the power losses of the devices at high-frequency operation, stating that semiconductors with greater mobility and breakdown electric fields result in reduced power losses [9].

Table 1. Material properties of crucial semiconductor materials used in power electronics.

Property Name	Si	GaAs	SiC	4HSiC	GaN	AlN	Diamond
Thermal expansion ($\times 10^6$ °C)	2.6	5.9	4.7	4.2	5.6	4.5	0.08
Density (g/cm ³)	2.328	-	3.210	3.211	6.095	3.255	3.515
Melting point (Co)	1420	-	3.210	2830	3530	-	4000
Bandgap (eV)	1.1	1.43	2.2	3.26	3.45	6.2	5.45
Electron velocity ($\times 10^7$ s ⁻¹)	1.0	1.0	2.2	2.0	2.2	-	2.7
Breakdown ($\times 10^5$ Vcm ⁻¹)	3	6	20	30	>10	-	100
Dielectric constant	11.8	12.5	9.7	9.6	9	8.5	5.5
Carrier mobility (cm ² N-s) electrons/holes	1500/600	8500/400	1000/50	1140/50	1250/850	-	2200/1600
BFOM (relative to Si)	1.0	15.7	4.4	-	24.6	-	101

Among power convertor topologies, flyback is one of the most commonly used topologies. It is essentially a buck–boost topology that is isolated by a transformer as the storage inductor. Moreover, the transformer not only provides isolation, but also, by varying the turn-ratio, the input and output voltages can be regulated. Flyback topologies are well-suited for high-output voltages with high peak currents.

An experimental comparison between a commercially available enhancement-mode GaN FET and two Si-based MOSFETs is presented in [10], discussing the power densities, switching speeds, temperature stabilities, on-state resistance, conduction and switching losses, and the reduction in the die size with the introduction of GaN. The use of GaN in power electronics is reported in [11], relating the impact ionization coefficients for holes and electrons, along with a comparison of the breakdown electric field with that of Si and silicon carbide (SiC). A study on the properties and advantages of GaN, along with the characteristics and reliability of GaN-based transistors in next-generation power converters, is discussed in [12,13]. The basic structure of AlGaIn/GaN high electron mobility transfer (HEMT), along with a comparison of its properties with other technologies, is presented in [14]. R. Chua et al. claims that the GaN-based power switches promise a 1000-times improvement over the current Si technology. Furthermore, a study in [15] reports that GaN-based, vertical device structures have the potential to substantially improve chip-area utilization, resulting in power switches with a much higher current rating and lower on-resistance. A review of power management solutions using linear charge pump topologies for upcoming technological challenges, such as IoT nodes, is reported in [16]. A comparative study of behavioral model for charge pumps operating in a wide-range of frequencies has been presented in [17]. D. Reusch et al. [18] investigates the switching operation of GaN

devices at a high frequency of 1.2 MHz in soft-switching applications. In [19], the reasons for the current drops and zero voltage switching (ZVS) loss in an active-clamp flyback converter is explained at 1 MHz switching frequency. The comparison of two high-efficiency, high-power-density designs of chargers in a quasi-resonant flyback and an active-clamp flyback topology is presented in [20]. While considering efficiency, [21] employs the use of a high switching-frequency to achieve a high-power-density of 177 W/inch³ and a maximum efficiency of up to 96.4%. The power-conversion efficiency of three different cascode GaN HEMT E-mode power modules in a DC-to-DC flyback converter topology is investigated in [22]. Considering line commutated converter (LLC) circuits, [23] reports an efficiency of 97.5% achieved when using GaN, in comparison with Si-based converters offering an efficiency in the range of 96.1%. A comprehensive review on LLC resonant converters using GaN HEMT switches instead of Si MOSFETs is presented in [24], whereas [25] investigates switching efficiency for dual-active-bridge converter prototypes with Si and GaN devices at 1 MHz, reporting an efficiency of 93%.

This research presents a comparative analysis of a GaN and Si-based MOSFETs for power and switching efficiency in an active clamp DC-to-DC flyback converter. The utilized flyback converter is widely used for PWM operations, considering its efficiency and simple design. The efficiencies are investigated in high frequency-switching up to 1 MHz and step-down operations. The operation of the topology is analyzed under different input conditions, as well as different types of resistive–inductive–capacitive (RLC) loads. Different features of the flyback converter, such as switching speed, switching efficiency, on-state resistance, and power consumption, are part of the discussion. The proposed work emphasizes the use of GaN-based devices for compact power-switching converters. The main concerns in the emerging power-converter circuits, such as high-power-density and efficiency improvements, are discussed.

2. Methodology

To calculate the power efficiency and losses in GaN-based FET in DC-to-DC converters, an active-clamp flyback-converter circuit topology (shown in Figure 1) was designed and simulated in LTspice software. A flyback is a simple DC-to-DC or AC-to-DC converter which consists of a transformer that stores the energy when the current is passing through the circuit and releases it when the power is removed. A flyback topology was chosen, keeping in mind its characteristics, to be used for both step-up and step-down operations. Besides that, it is extremely favorable for both isolating and non-isolating applications. Current handling capability at the secondary side of the circuit is also a major focus in this topology with varying input voltage. The presence of a transformer in the chosen topology provides complete isolation between the input and the output. Here, MOSFET functions as an ON/OFF switch in the circuitry which can magnetize and demagnetize the transformer. Two different models of MOSFET, i.e., pure Si (IXTK 200N10P) and GaN (EPC2001) [25], are used as switching devices in the circuit. Moreover, different rectifiers and filters are used at the output stage. In the final stage, the results of the flyback converter with both of the above-mentioned MOSFET switches are compared in regard to the power and switching efficiency of the circuits. The sizes of the switching devices and the switching speeds are also part of the discussion. The utilized topology with GaN FET, its efficiency calculation, and losses are briefly discussed in the upcoming sections.

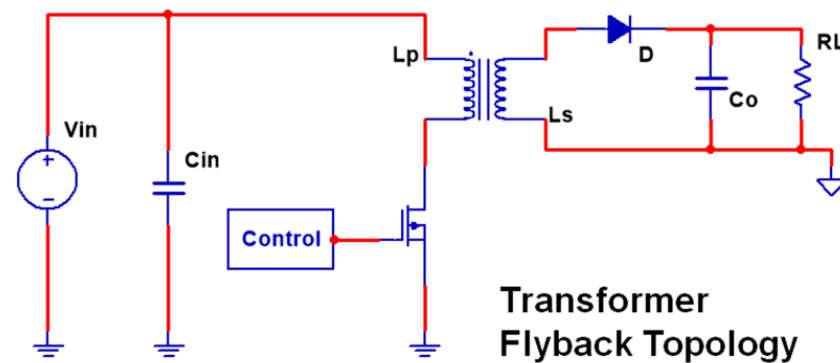


Figure 1. DC-to-DC converter with flyback topology.

2.1. DC-to-DC Flyback Converter

The flyback converter produces a regulated output with control over the magnitude of the input voltage. The flyback converter also allows the possibility of using pulse width modulation (PWM) in a continuous mode of operation, as shown in Figure 2. It also allows the usage of feedback loops to maintain good control over the output voltage, even if the input current and voltage are changing. Figure 2a shows the circuit topology with a GaN-based FET as a switching device. Moreover, a PWM input to the circuit, a DC input to the transformer, a rectifier, and a filter before the DC output are shown. The internal structure of the FET with a layer of GaN and an isolation layer is shown in Figure 2b. The performance characteristics of the flyback converter include ripple voltage, efficiency, frequency, size of the device, and weight.

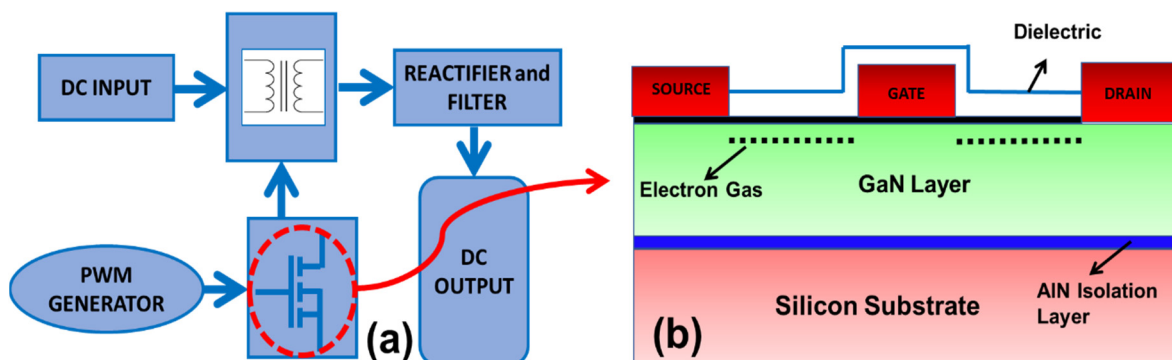


Figure 2. (a) Block diagram of flyback topology with PWM as input to the switch; (b) the internal structure of a GaN FET.

A schematic view of the simulated circuit, with an indication of input voltage source (V1), switching transistor (M1), PWM generator (V2), transformer, capacitors (C1 and C2), diodes (D1 and D2), and the load at the out, is shown in Figure 3. The current in the isolated transformer cannot flow simultaneously in both the windings. When the transistor (M1) conducts, the diode (D1) is reverse biased; thus, the primary winding acts as an inductor connected to the input source, resulting in energy storage in the flyback transformer. When the transistor (M1) turns off, the current stops flowing in the primary coil of the transformer; however, at the same time, magnetizing current flows in the secondary winding, forward biasing the diode (D1). Hence, the stored energy in the magnetic field of the transformer is transferred to the load. A 24 V DC voltage source is used at the input, and the circuit steps down the voltage to 7 Vs at the output. The GaN-based MOSFET (M1) performs the primary role in the circuit, where the gate signal is being controlled by PWM. The square wave generated by the PWM generator (V2) maintains a fixed frequency, regardless of the power transferred to the load. The sharp rising pulse saturates M1, bringing the collector voltage of the transistor to almost ground. After the MOSFET switches ON, the primary

side (L1) of the transformer stores the energy, and the capacitor acts as an open circuit, resulting in no current flow across it. The value of the current linearly increases in the coil for a time period (t) due to the magnetizing inductance. At the same time, the diode (D2) at the output opposes the current flow at the load. The voltage at the load (V_{Load}) current through the capacitor (C1) and gate current of (M1) are expressed as:

$$V_{Load} = V1$$

$$I_{C1} = -\frac{V_L}{R}$$

$$I_{gate\ M1} = I$$

Here, V_L is voltage across load and R represents the load resistance.

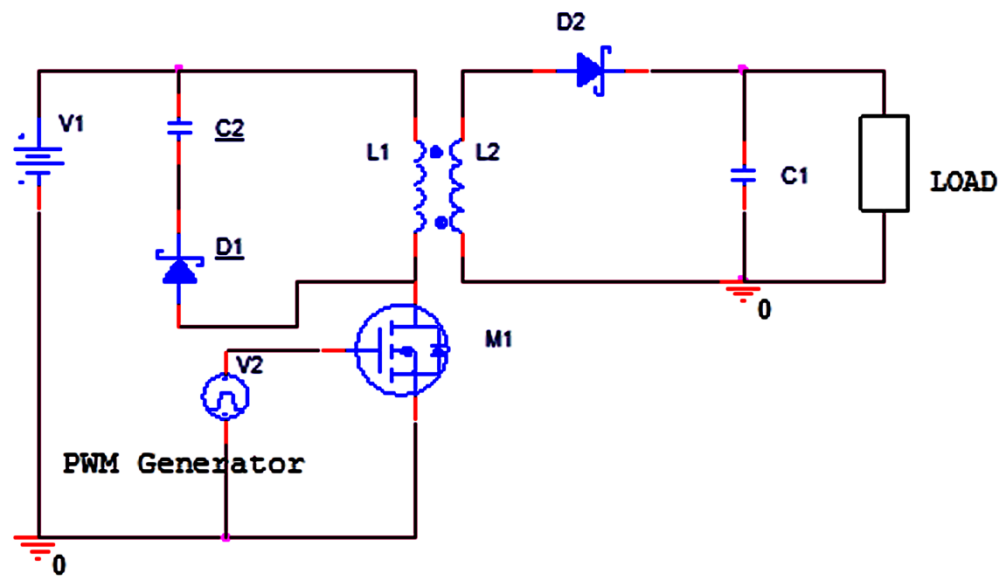


Figure 3. GaN-based active-clamp flyback converter topology with DC source, PWM generator, and load at the output.

When the MOSFET is switched OFF, the polarity of the transformer primary reverses, causing the flow of stored energy at the primary coil to the secondary, and ultimately to the load. As the current decreases in the primary coil, a voltage is induced in the secondary coil in the correct direction for the current to flow. This flyback effect increases the collector voltage to a greater value than the input supply voltage. The current can flow in either the primary or the secondary coil, but not simultaneously in both the coils. When the switch (M1) is off, the polarity of the inductor reverses, and the current flows through the diode (D2), charging the capacitor in a transient state. The V_{Load} and I_{C1} are given by:

$$V_{Load} = \frac{V}{n}$$

$$I_{C1} = \frac{I}{n} - \frac{V}{R}$$

where n represents the number of turns of the transformer.

2.2. Efficiency

The power efficiency η of the circuit is given as a ratio of the output power P_{out} to the input power P_{in} . where the input power is represented as the sum of ($V_{out} \times I_{out} + Power\ losses$) and the output power as ($V_{out} \times I_{out}$):

$$\eta = \left(\frac{P_{out}}{P_{in}} \right) \times 100$$

$$\eta = \frac{V_{out} * I_{out}}{V_{in} * I_{in}} \times 100$$

$$\eta = \frac{V_{out} \times I_{out}}{V_{out} * I_{out} + Power\ losses} \quad (1)$$

where the total power losses in the circuit include conduction losses, switching losses, and leakage inductance losses.

2.3. Losses

The transformer leakage inductance losses are related to the leakage inductance that exists between the primary and the secondary coil. The amount of the energy stored by the inductor coil is given by

$$P_e = \frac{1}{2} L_e I_p^2 f_{sw}$$

where f_{sw} is the switching frequency, L_e is the value of inductor, and I_p is the current in the primary coil. The total losses of the windings of the transformer can be given as:

$$P_{1w} = I_{1DC}^2 R_{1DC} + I_{1AC}^2 R_{1AC}$$

$$P_{2w} = I_{2DC}^2 R_{2DC} + I_{2AC}^2 R_{2AC}$$

$$P_w = P_{1w} + P_{2w} \quad (2)$$

where $I_{1DC}^2 R_{1DC}$ represents the dissipated DC power, and $I_{1AC}^2 R_{1AC}$ shows the dissipated AC power through the transformer.

Diode conduction losses are caused by the semiconductor's forward voltage and are I²R losses. MOSFET switching losses are directly related to its operating frequency.

2.3.1. MOSFET Conduction Losses

The power dissipation when the transistor is ON is calculated by

$$P_{con} = \frac{1}{T} \int_0^{T_{on}} i^2(t) R_{DS(on)}(t) \cdot dt$$

$$T = \frac{1}{f_{SW}}$$

where P_{con} is the conduction losses, and $R_{DS(ON)}$ is the resistance of the MOSFET when it is switched ON, which is temperature-dependent, whereas I is the current passing through the MOSFET, and T_{on} shows the ON time.

2.3.2. MOSFET Switching Losses

MOSFET switching losses can be calculated in both ON and OFF states and are mathematically expressed by $P_{SW(ON)}$ and $P_{SW(OFF)}$ as shown below:

$$P_{SW(ON)} = f_{SW} \int_0^{T_{ON}} i_d(t) V_{ds}(t) \cdot dt$$

$$P_{SW (ON)} = f_{SW} \left[\frac{V_{ds (max)} I_d (max) t_{ON}}{6} \right]$$

Here, V_{ds} is the maximum drain-to-source voltage across the transistor, and I_d shows the maximum drain current.

Similarly, when the transistor is OFF, the $P_{SW (OFF)}$ can be expressed as:

$$P_{SW (OFF)} = f_{SW} \left[\frac{V_{ds (max)} I_d (max) t_{OFF}}{6} \right]$$

Hence, the total loss can be calculated by combining the above two expressions for $P_{SW (ON)}$ and $P_{SW (OFF)}$, which is given as:

$$P_{SW (total)} = \frac{V_{ds (max)} I_d (max) (t_{ON} + t_{OFF}) f_{SW}}{6} \quad (3)$$

The gate charge losses are produced by charging up the gate and then the drainage of the total charge to the ground (QG) at every cycle. The gate charge losses are directly proportional to the frequency:

$$Eg = QG \times V_{ds} \times f_{SW} \quad (4)$$

3. Results and Discussion

The performance of the flyback converter topology is tested for both GaN- and Si-based MOSFET switches, and a comparative analysis is presented. The efficiency of the topology is calculated by adding different types of loads, i.e., resistance, inductive, capacitive, and RLC at the output. The utilized step-down transformer takes 24 V input, and the output is almost two-times less than the input voltage. A PWM signal with period of 1 μ s, with a rise and fall time of 0.01 ns, V_{on} of 5 V, and ON time of 0.25 μ s, is used as an input for the gate of a GaN FET. The comparative analysis between a Si-based MOSFET switch and a GaN FET switch is performed for different circuit-load configurations, which are discussed in the following sections.

3.1. Open Circuit Configuration

In the first step, an open-circuit configuration is simulated with the load disconnected, as shown in Figure 4. The no-load output responses of the above-discussed circuit for switching devices such as GaN FETs and Si MOSFETs are shown in Figures 5 and 6, respectively. The results show voltage responses when the current changes in the primary coil, and due to mutual induction, a current flow occurs in the secondary coil. With no load condition, the capacitor (C1) placed in parallel to the output continues charging, and the time it requires to reach a steady state depends on the value of the capacitor. As the voltage continues rising at the input of the capacitor, the capacitor continues charging. The numerically calculated curves show a continuous rise in the voltage of the capacitor during charging; however, practically, the capacitor has a limited capacity. The output voltage can be calculated at the steady-state value of the voltage curve, where a step-down process can be seen. Moreover, the open-circuit response of the Si MOSFET in Figure 6 depicts the no-response behavior of the Si MOSFET at the given frequency.

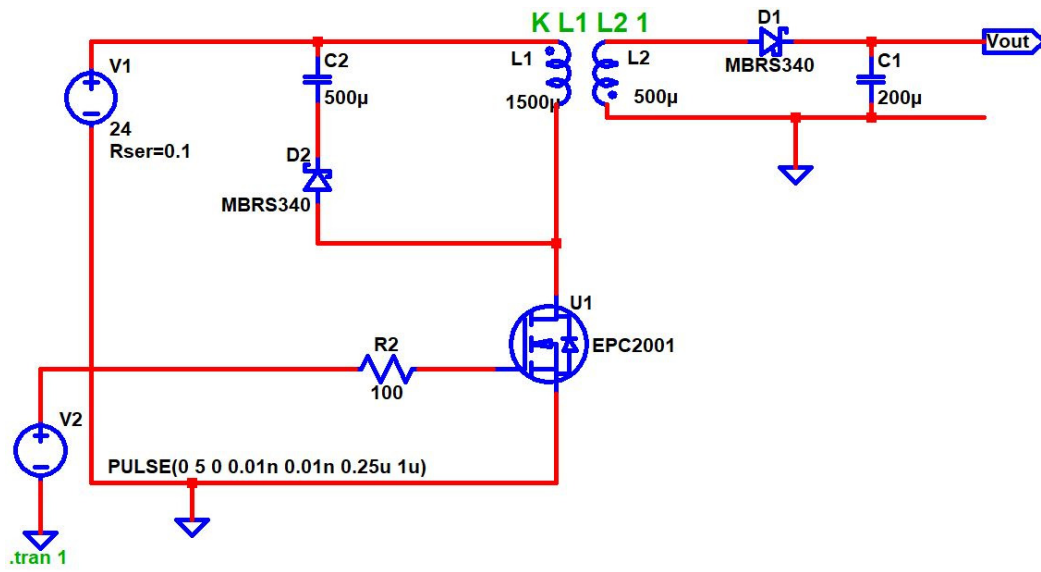


Figure 4. Open-circuit configuration of active flyback DC-to-DC converter.

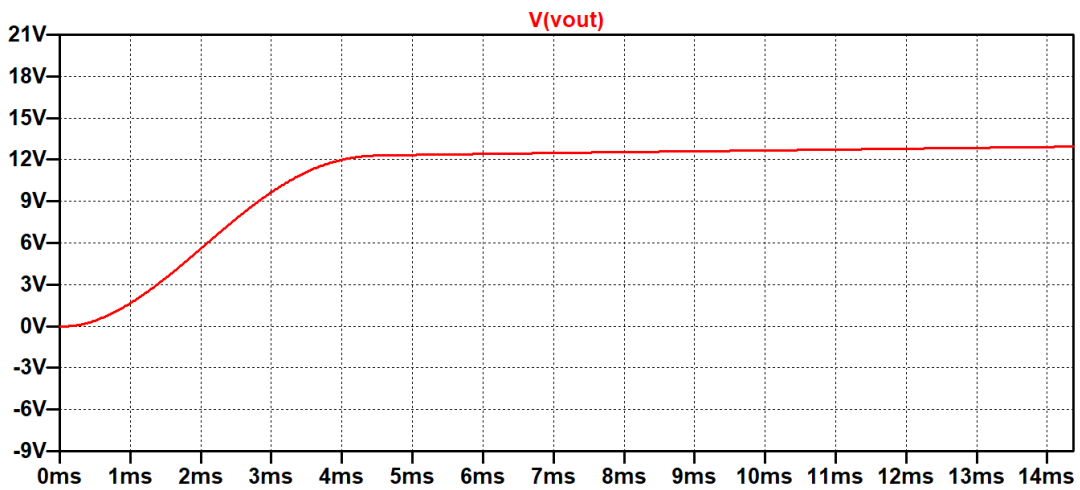


Figure 5. The output voltage response of GaN-FET-based switch for an open-circuit configuration.

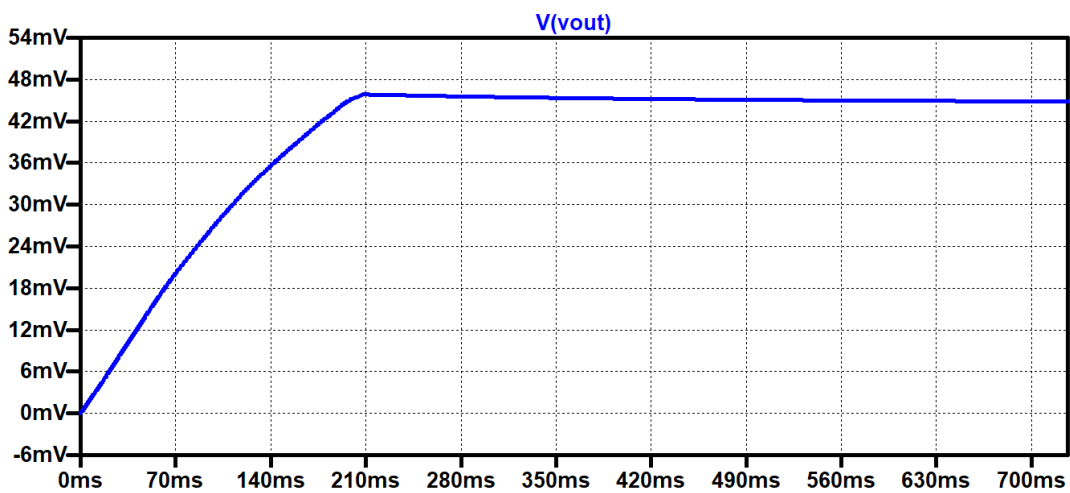


Figure 6. The output voltage response of Si-MOSFET-based switch for an open-circuit configuration.

3.2. Resistive Load Configuration

The circuit configuration with a resistive load of 10 KΩ is shown in Figure 7. The output waveform for a GaN-based switch in Figure 8 shows the effect of resistive load at the output, where the current passing through the primary winding of the transformer is varying the voltage on the secondary side due to mutual induction. This change in voltage is thus passed on directly to the output resistor passing through the diode (D1), which can only resist for a specific time by increasing to the maximum voltage of 8 V and then dropping to the negative minimum value. As the output loop is grounded, the voltage thus continues swinging between the peak values during the switching process and cannot sustain a constant level. Both current and voltage are in phase in this configuration. In comparison to a GaN switch, the voltage response of a Si MOSFET with a resistive load is depicted in Figure 9, where the peak values are restricted between values of around −65 mV and 85 mVs, and the switching frequency cannot be properly followed at the output.

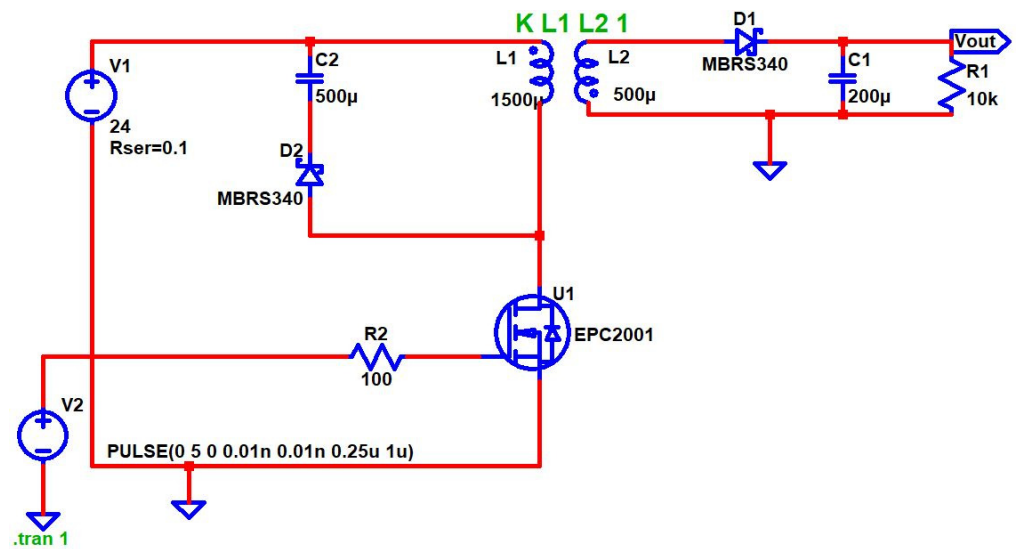


Figure 7. DC-to-DC flyback converter circuit response with a resistive load.

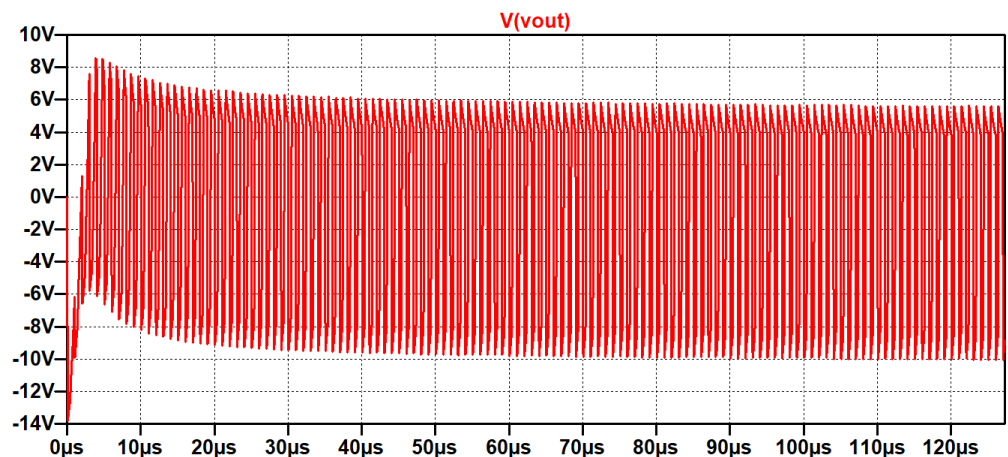


Figure 8. The output voltage response of circuit with GaN switch and resistive load configuration.

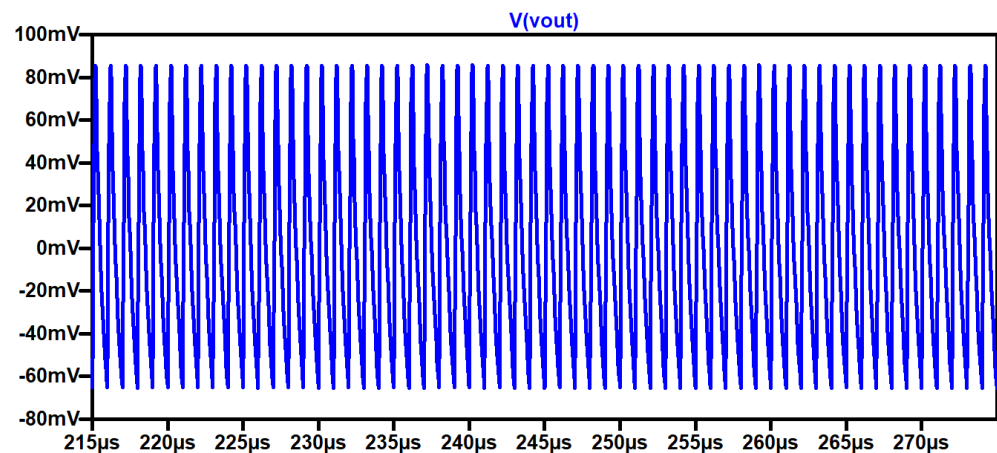


Figure 9. The output voltage response of circuit with Si MOSFET as switch and resistive load configuration.

In the circuit configuration shown in Figure 10, the value of load resistor (R1) is reduced from 10 KΩ to 5 Ω to check the frequency response of the circuit. This reduction in the value of the load resistor happens to ensure that the maximum current flows through the load. The mutual induction causes the variation of current on the secondary side, producing a voltage at the output which appears at the load (R1) by ensuring maximum current through it. The waveform in Figure 11a shows that the voltage increases due to the charging of the output capacitor, and it appears in the form of a transient spike of 11 V. At this point, the capacitor charges fully, and the resistor connected in parallel with the capacitor (C1) maintains the output voltage constant at 7 V. The initial transient peak of 11 V and a steady-state of 7 V is achieved due to the nature of the output load.

The output waveform in Figure 11b shows the value of both the current and the voltage simultaneously. The output efficiency is calculated by measuring the input/output voltage and the current, as shown in Equation 1. The output voltage is measured to be 7.2 V, and the output current is 1.4 A. By equating the values of the input and the output in the equation, the efficiency of the flyback converter is calculated to be 99.6%. The power of the converter can also be calculated with the resultant voltage and current values. In keeping with the comparative study, the output voltage response of the converter is also measured for a Si-based switch, as depicted in Figure 12. It can be observed that the Si-based switch is unable to follow the frequency and hence limits the output to a few mV, which limits the circuit to an almost no-response, as compared to a GaN switch.

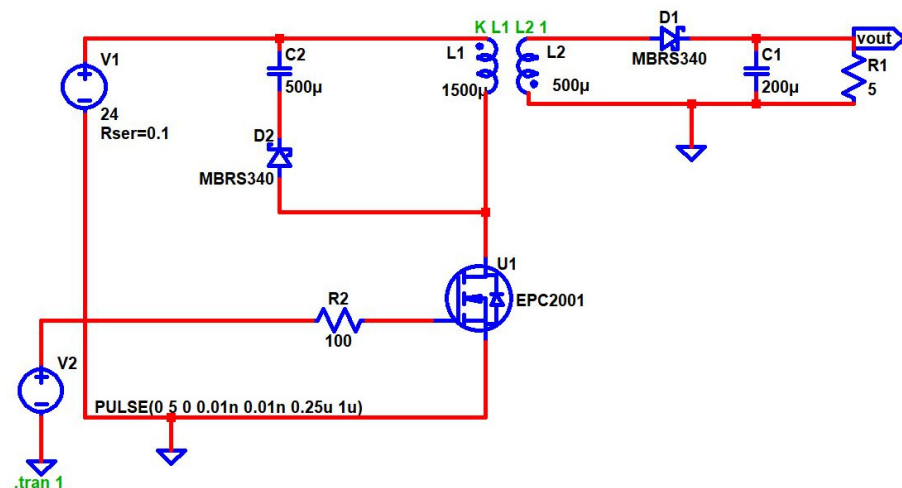


Figure 10. DC-to-DC flyback converter with resistive load of 5 Ω.

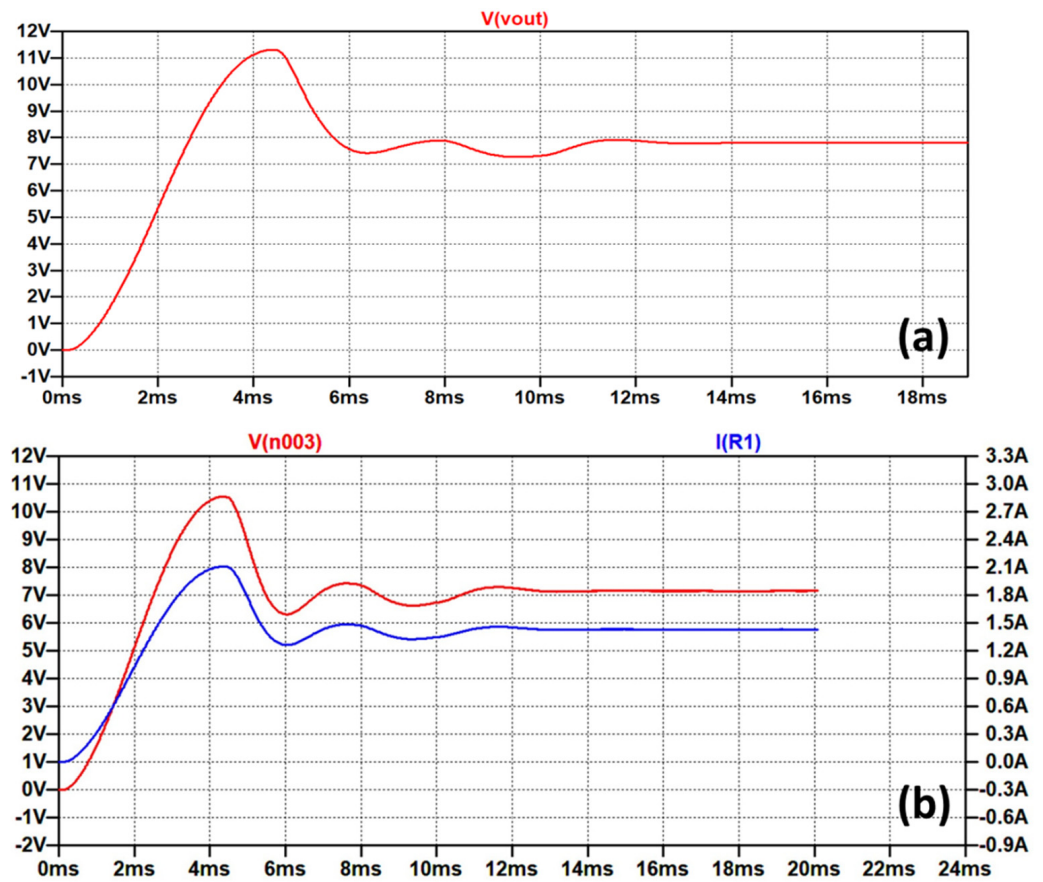


Figure 11. (a) The output-voltage response with resistive load; (b) the output current and voltage response of the circuit with resistive load.

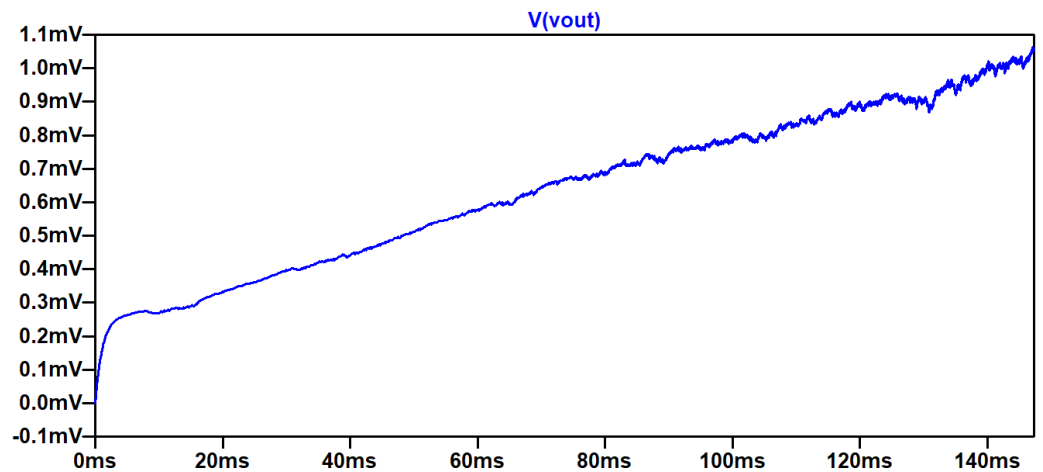


Figure 12. The output-voltage response of the circuit with Si MOSFET as switch and RC load at output.

3.3. Inductive Load Configuration

Figure 13 shows the flyback converter topology with an inductive load ($L3$) of $100\ \mu\text{H}$ and a capacitor ($C1$) connected in parallel. The values of the components are chosen to achieve a maximum output and asper convention, the value of output capacitor ($C1$) is kept high to reduce the ripple effect at the output. Output waveforms for current and voltage are plotted together in Figure 14. A parallel combination of capacitor and inductor makes an LC tank filter, and the output efficiency can be calculated accordingly.

As soon as the voltage across the inductor reaches zero, the current starts increasing, which indicates the fact that the variation in the current is inside the inductor, which keeps it charging. The output waveform shows a gradual increase in current from 0 to 24 A. It is important to mention here that the simulation results show a continuous increase in the value of the current, which is not practically possible due to the physical limitations of the components. On the other hand, the voltage shows a transient spike of 0.8 V as the capacitor charges, but it fails to sustain its value, and after some time, it drops to a steady-state value around 360 mV. As a comparative study, the response of the circuit for the LC load and a Si MOSFET switch is shown in Figure 15. The small positive and negative voltage peaks show that the Si switch is not capable of providing the desired output at the given frequency.

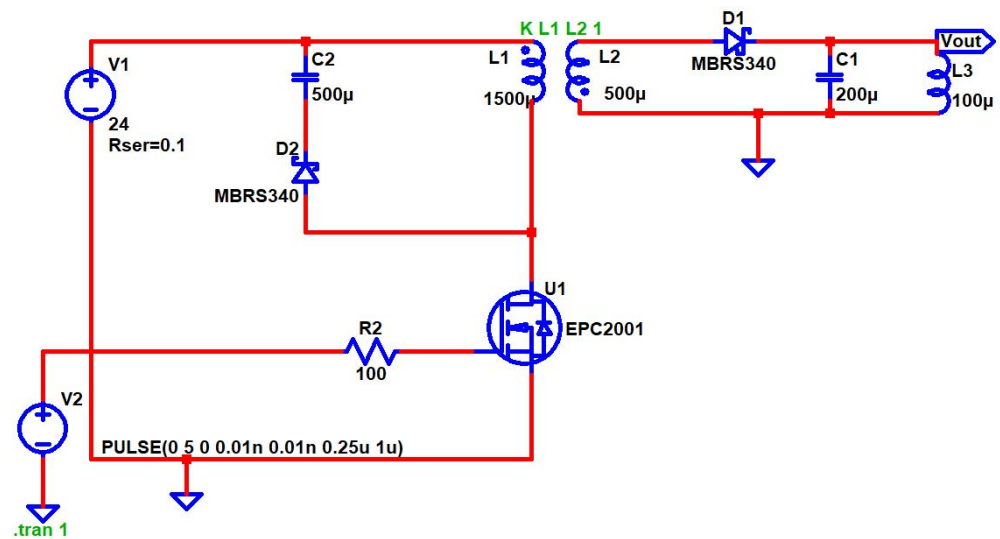


Figure 13. DC-to-DC flyback converter with inductive load configuration.

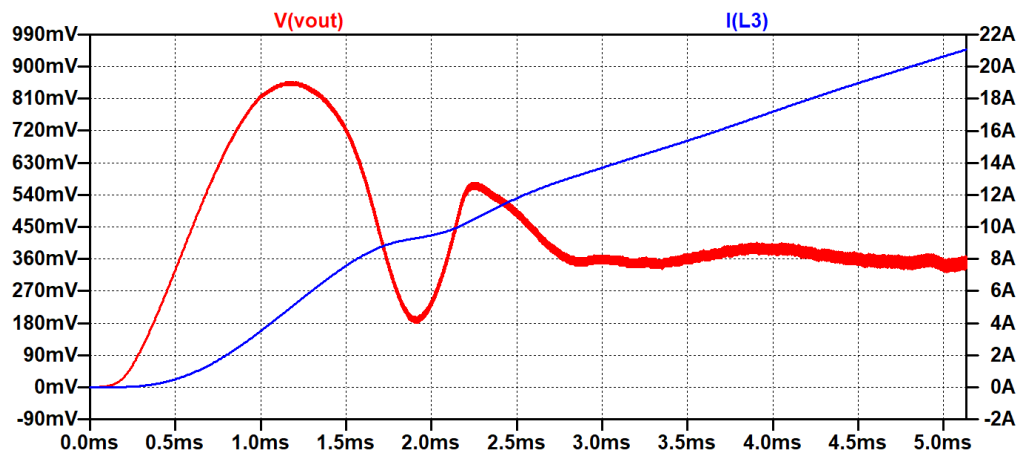


Figure 14. The output voltage and current response of the circuit with GaN switch and LC load.

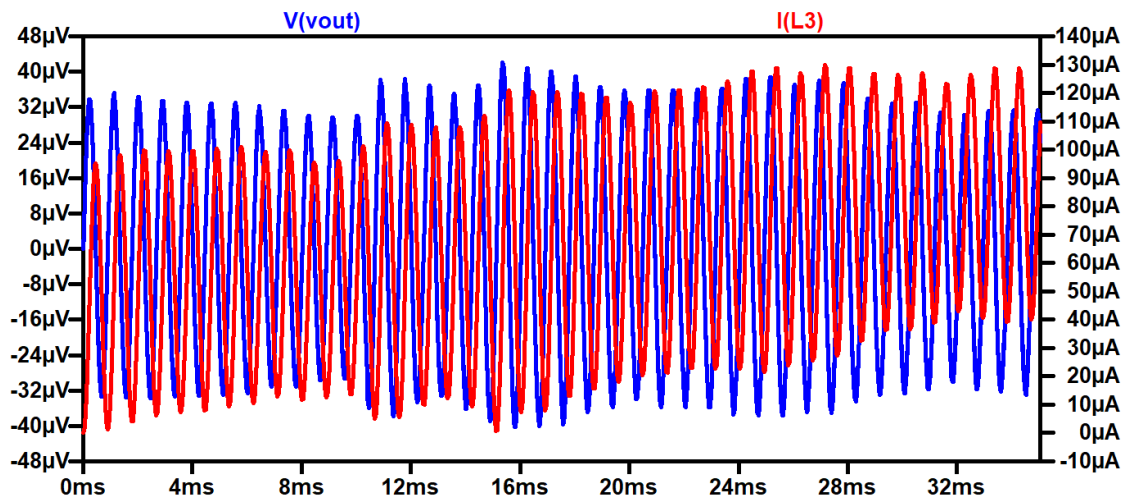


Figure 15. The output voltage and current response of the circuit with Si-MOSFET-based switch and LC load.

3.4. RLC Load Configuration

The circuit topology with an RLC load is shown in Figure 16 with L3 of 100 μ H, R1 with 5 Ω , and C1 of 200 μ F. The output waveform in Figure 17a shows the response of the converter for an RLC series circuit as the load. It can be observed that, in this case, the output voltage response is similar to that of the resistive load. The capacitor (C1) charges when the diode (D1) reaches a maximum peak of 10 V. As the voltage peak starts to fall and the inductor acts as a short circuit for DC current, the presence of the load resistor (R1) prevents the further drop of voltage and brings it to a steady state value of 7 V. However, there is still a possibility of voltage fluctuations due to the LC behavior of the circuit. The presented circuit topology offers an efficiency of 99.6%. Figure 17b shows the response of the current at both the input and the output sides of the circuit. The output current I(L3) current across the inductor (L3) is maintained at 1.4 A. The current I(L1) indicates the input current through the coupled inductor (L1), and the mutual induction depends on the turn ratio of the transformer. A peak of -72 V in the graph indicates that during the off time of the switch (U1), a voltage builds up across the switch, which is the algebraic sum of the input voltage and the output voltage developed at the end of the coupled inductor (L1).

For the sake of comparison, the output response of the circuit with a Si MOSFET switch with an RLC load is shown in Figure 18. It can be seen that the output voltage of a few mV appears at the output, which proves that the Si-based switch is not capable of following the switching frequency of 1 MHz.

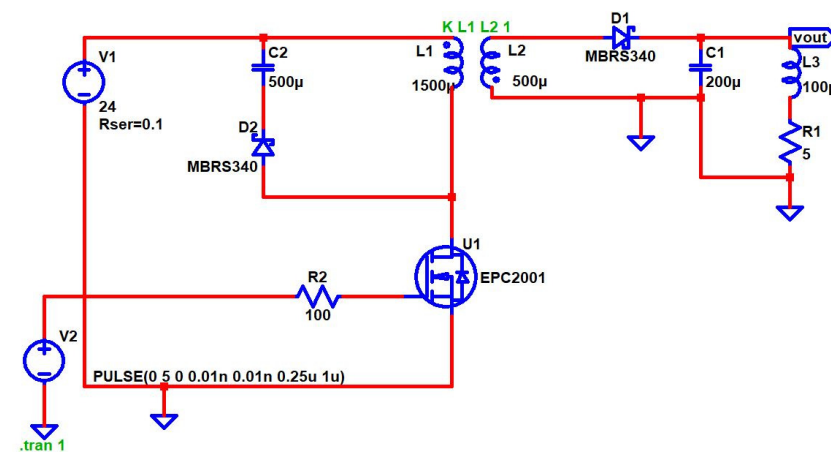


Figure 16. GaN-switch-based DC-to-DC flyback converter with RLC load configuration.

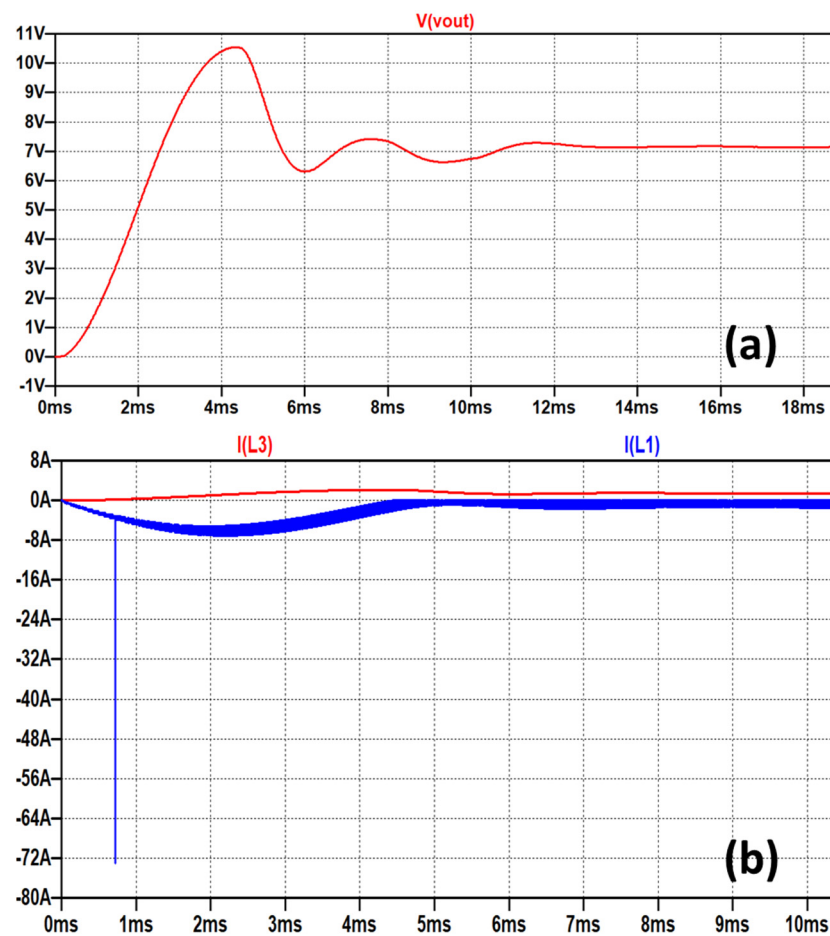


Figure 17. (a) The output voltage response with GaN switch and RLC load; (b) the input and output current responses with GaN switch and RLC load.

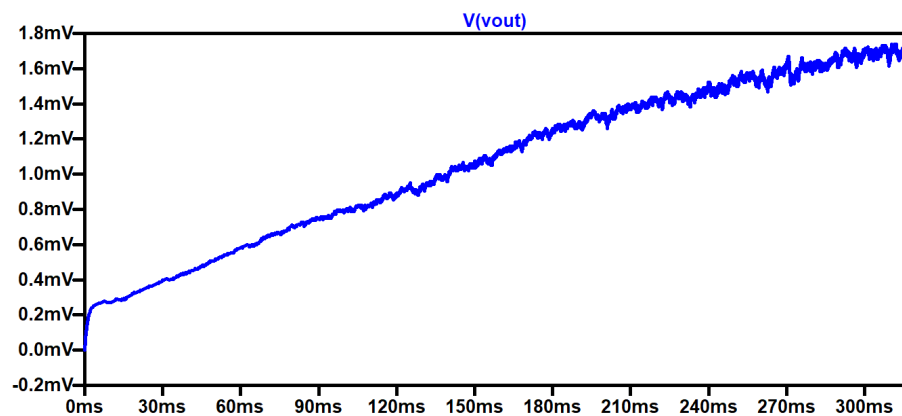


Figure 18. The output-voltage response of the circuit with Si-MOSFET-based switch and RLC Load.

3.5. Comparative Analysis of Output Parameters

Table 2 gathers the comparative results of both the GaN- and Si-based switches for different kinds of losses in the circuit, including switching, conduction, and induction losses, and the total power-efficiency of the convertor. The results are calculated using Equations (1)–(5), and it can be concluded that the Si MOSFET is unable to work on the frequency of 1MHz. Only a current in the range of few mAs is able to flow through the Si MOSFET, which produces no drain current, and ultimately, the net efficiency of the converter using the Si MOSFET is close to zero.

Table 2. Losses and efficiency calculation table.

S. No.	Parameters	Si Power MOSFET (W) (IXTK 200N10P)	GaN MOSFET (W) (EPC2001C)
1	Switching Loss at ON State (W)	0	0.628
2	Switching Loss at OFF State (W)	0	1.885
3	Total Switching Loss (W)	Not Working	2.513
4	Conduction Loss at ON State (W)	0.000000000004 approx. zero	0.420×10^{-3}
6	Total conduction loss at OFF state (W)	0.000000000008 approx. zero	0.840×10^{-3}
7	Inductive loss (W)	1.074	39.2 m
8	Total loss (W)	maximum	2.553
9	Power-Efficiency of Converter (%)	0.0041	99.6

4. Conclusions

In this article, a comparative study of the operation of MOSFET switches based on two different materials, i.e., Si and GaN, is presented in a DC-to-DC active-clamp flyback converter for a step-down application. The output response of the circuit is investigated for different types of loads, such as R, RC, and RLC. From the results, it can be concluded that the operating parameters of GaN-based switches are far more superior to ordinary Si switching devices, with the benefits of having high V_{DS} and a much lower $R_{DS(ON)}$, typically in the range of 7 m Ω . The proposed topology offers the improved efficiency of this DC-to-DC converter by reducing the losses concerned with the MOSFET switch via the use of GaN as the gate material. The absence of body diodes in the GaN MOSFET is its unique property that results in a reduction of reverse recovery loss. Comparative results with different loads are presented for the switching frequency in the range of 1 MHz and above. The Si-based MOSFET switch is unable to follow the mentioned frequency range, and therefore, the current flow through the switch is nearly zero, creating a nominal level of voltage at output, as compared to the GaN-based switch. Hence, with the introduction of the GaN switch, the power conversion efficiency is calculated to be 99.6% in the proposed topology, making GaN-based converters much more efficient than conventional power converters. The high-frequency operation of the converter increases the power density of the device, thereby reducing the component size and offering much more compact circuit designs. The GaN-based devices are still categorized as a new technology that can perform well on higher frequencies, and they lead the way for improvement in the frequency response of other discrete components being used in power electronics.

Author Contributions: Conceptualization, O.A. and Y.K.; methodology, O.A., Y.K. and M.A.B.; software, O.A. and Y.K.; validation, Y.K. and M.A.B.; formal analysis, Y.K. and M.A.B.; investigation, O.A. and Y.K.; resources, Y.K. and M.A.B.; data curation, O.A. and Y.K.; writing—original draft preparation, O.A. and Y.K.; writing—review and editing, Y.K., S.N.K., N.L.K. and M.A.B.; visualization, O.A. and Y.K.; supervision, Y.K. and M.A.B.; project administration, Y.K., M.A.B., S.N.K. and N.L.K.; funding acquisition, Y.K. and M.A.B. All authors have read and agreed to the published version of the manuscript.

Funding: This work was financially supported by the Ministry of Science and Higher Education of the Russian Federation under the Samara National Research University (project FSSS-2021-0016) in the overview and numerical parts and under the FSRC “Crystallography and Photonics” of the Russian Academy of Sciences (the state task No. 007-GZ/Ch3363/26) in the part of theoretical analysis.

Data Availability Statement: Not applicable.

Acknowledgments: The authors are grateful to all of the group members of the Embedded Systems research group at BUIITEMS Quetta who made this research possible.

Conflicts of Interest: The authors declare no conflict of interest.

References

1. Baliga, B.J. Evolution of MOS-bipolar power semiconductor technology. *Proc. IEEE* **1988**, *76*, 409–418. [CrossRef]
2. Tajalli, A.; Meneghini, M.; Besendörfer, S.; Kabouche, R.; Abid, I.; Püsche, R.; Derluyn, J.; Degroote, S.; Germain, M.; Meissner, E.; et al. High breakdown voltage and low buffer trapping in superlattice gan-on-silicon heterostructures for high voltage applications. *Materials* **2020**, *13*, 4271. [CrossRef] [PubMed]
3. Baliga, B.; Sears, A.; Barnicle, M.; Campbell, P.; Garwacki, W.; Walden, J. Gallium arsenide Schottky power rectifiers. *IEEE Trans. Electron Devices* **1985**, *32*, 1130–1134. [CrossRef]
4. Baliga, B.J. *Fundamentals of Power Semiconductor Devices*; Springer: New York, NY, USA, 2008.
5. Baliga, B.J. *Advanced Power MOSFET Concepts*; Springer Science & Business Media: New York, NY, USA, 2010.
6. Yoder, M.N. Wide bandgap semiconductor materials and devices. *IEEE Trans. Electron Devices* **1996**, *43*, 1633–1636. [CrossRef]
7. Denbaars, S.P. Gallium-nitride-based materials for blue to ultraviolet optoelectronics devices. *Proc. IEEE* **1997**, *85*, 1740–1749. [CrossRef]
8. Baliga, B.J. Gallium nitride devices for power electronic applications. *Semicond. Sci. Technol.* **2013**, *28*, 074011. [CrossRef]
9. Khoshzaman, S.; Hahn, I. A Performance Comparison of GaN FET and Silicon MOSFET. In Proceedings of the 2021 22nd IEEE International Conference on Industrial Technology (ICIT), Valencia, Spain, 10–12 March 2021; Volume 1, pp. 127–133.
10. Khan, M.A.; Simin, G.; Pytel, S.G.; Monti, A.; Santi, E.; Hudgins, J.L. New developments in gallium nitride and the impact on power electronics. In Proceedings of the 2005 IEEE 36th Power Electronics Specialists Conference, Dresden, Germany, 16 June 2005; pp. 15–26.
11. Meneghini, M.; De Santi, C.; Abid, I.; Buffolo, M.; Cioni, M.; Khadar, R.A.; Nela, L.; Zagni, N.; Chini, A.; Medjdoub, F.; et al. GaN-based power devices: Physics, reliability, and perspectives. *J. Appl. Phys.* **2021**, *130*, 181101. [CrossRef]
12. Scott, M.J.; Fu, L.; Zhang, X.; Li, J.; Yao, C.; Sievers, M.; Wang, J. Merits of gallium nitride based power conversion. *Semicond. Sci. Technol.* **2013**, *28*, 074013. [CrossRef]
13. Mishra, U.K.; Parikh, P.; Wu, Y.F. AlGaIn/GaN HEMTs—an overview of device operation and applications. *Proc. IEEE* **2002**, *90*, 1022–1031. [CrossRef]
14. Chu, R. GaN power switches on the rise: Demonstrated benefits and unrealized potentials. *Appl. Phys. Lett.* **2020**, *116*, 090502. [CrossRef]
15. Reusch, D.; Strydom, J. Evaluation of gallium nitride transistors in high frequency resonant and soft-switching DC–DC converters. *IEEE Trans. Power Electron.* **2014**, *30*, 5151–5158. [CrossRef]
16. Ballo, A.; Grasso, A.D.; Palumbo, G. A review of charge pump topologies for the power management of IoT nodes. *Electronics* **2019**, *8*, 480. [CrossRef]
17. Ballo, A.; Bottaro, M.; Grasso, A.D.; Palumbo, G. Regulated charge pumps: A comparative study by means of verilog-AMS. *Electronics* **2020**, *9*, 998. [CrossRef]
18. Meng, W.; Li, L.; Zhang, F.; Shu, J. Soft-switching Resonant Active Clamp Flyback Converter based-on GaN HEMTs for MHz High Step-up Applications. In Proceedings of the 2021 IEEE Workshop on Wide Bandgap Power Devices and Applications in Asia (WiPDA Asia), Wuhan, China, 25–27 August 2021; pp. 57–62.
19. Dey, S.; Ray, M.B.; Soni, H.; Ghosh, R.; Shah, M. Comparison between Quasi-Resonant and Active Clamp Flyback topologies for GaN-based 65W Wall Charger Application. In Proceedings of the 2021 IEEE Applied Power Electronics Conference and Exposition (APEC), Phoenix, AZ, USA, 14–17 June 2021; pp. 1809–1814.
20. Huang, D.; Gilham, D.; Feng, W.; Kong, P.; Fu, D.; Lee, F.C. High power density high efficiency dc/dc converter. In Proceedings of the 2011 IEEE Energy Conversion Congress and Exposition, Phoenix, AZ, USA, 17–22 September 2011; pp. 1392–1399.
21. Wu, C.-C.; Liu, C.-Y.; Anand, S.; Chieng, W.-H.; Chang, E.-Y.; Sarkar, A. Comparisons on Different Innovative Cascade GaN HEMT E-Mode Power Modules and Their Efficiencies on the Flyback Converter. *Energies* **2021**, *14*, 5966. [CrossRef]
22. Zhang, W.; Long, Y.; Zhang, Z.; Wang, F.; Tolbert, L.M.; Blalock, B.J.; Henning, S.; Wilson, C.; Dean, R. Evaluation and comparison of silicon and gallium nitride power transistors in LLC resonant converter. In Proceedings of the 2012 IEEE Energy Conversion Congress and Exposition (ECCE), Raleigh, NC, USA, 15–20 September 2012; pp. 1362–1366.
23. Mortazavizadeh, S.A.; Palazzo, S.; Amendola, A.; De Santis, E.; Di Ruzza, D.; Panariello, G.; Sanseverino, A.; Velardi, F.; Busatto, G. High Frequency, High Efficiency, and High Power Density GaN-Based LLC Resonant Converter: State-of-the-Art and Perspectives. *Appl. Sci.* **2021**, *11*, 11350. [CrossRef]
24. Costinett, D.; Nguyen, H.; Zane, R.; Maksimovic, D. GaN-FET based dual active bridge DC-DC converter. In Proceedings of the 2011 Twenty-Sixth Annual IEEE Applied Power Electronics Conference and Exposition (APEC), Fort Worth, TX, USA, 6–11 March 2011; pp. 1425–1432.
25. Available online: https://epc-co.com/epc/Portals/0/epc/documents/datasheets/EPC2001C_datasheet (accessed on 15 February 2022).